

# RF Interference Cancellation for Microwave Thermometry

Joseph Dunbar<sup>#1</sup>, Gabriel Santamaría-Botello<sup>\$2</sup>, Zoya Popović<sup>#3</sup>

<sup>#</sup>Electrical Engineering, University of Colorado at Boulder, USA

<sup>\$</sup>Electrical Engineering, Colorado School of Mines, USA

<sup>1</sup>joseph.dunbar@colorado.edu, <sup>2</sup>gabriel.santamaribotello@mines.edu, <sup>3</sup>zoya.popovic@colorado.edu

**Abstract**— This paper presents a method for cancelling external interference in a passive medical sensor for internal body temperature measurements. In microwave thermometry, a radiometric receiver measures the black-body radiation emitted by tissues inside the body. At room temperature and with a few tens of MHz bandwidth, black body radiation has a power around -100 dBm. With such low signal strengths, any transmitter (intentional or not) in the environment becomes a source of RFI. To reduce error in radiometric measurements, a simple and computationally inexpensive method for interference cancellation based on an auxiliary antenna and receiver is presented. Using this technique, temperature fluctuations due to RFI are significantly improved, which have a standard deviation in the error temperature of 3.5 K and max of 56 K, down to 0.38 K and a max of 2 K.

**Keywords**— radio frequency interference, microwave thermometry, radiometer, correlation

## I. INTRODUCTION

Internal body temperature is an important metric for both medical diagnostics [1], [2], [3] and treatment [4]. Fig. 1 illustrates radiometric brain temperature measurements, which are useful for monitoring temperature during, e.g. cardiac surgery [5] or traumatic brain injury. The temperature of internal organs or layers of tissue can be measured by amplifying and detecting their radiated black body power. Previous work used various higher microwave frequencies, e.g. between 3 and 4 GHz in a portable radiometer [6], or as high as 45 GHz, where a radiometer with a horn antenna was used to obtain temperature body images reported to show the heart location [7]. The low giga-hertz frequencies (1.4 GHz) for tissue penetration, over a bandwidth of about 60 MHz [8] are a good compromise between depth of sensing and size of the near-field antenna probe used to receive the thermal noise. For a few tens of MHz receiving bandwidth, the total received power is about -100 dBm. At these low power levels, practically all wireless applications as well as unintentional RF radiators in the environment become a significant source of radio frequency interference (RFI). In Fig. 1, a single interfering signal is shown as an illustration.

Interference makes deploying microwave thermometry outside of shielded environments challenging [9]. For a wearable thermometer used for monitoring, the hardware is limited in power, size, and cost. This in turn limits computational resources allocated to suppressing interfering signals. Here we present a simple technique for interference cancellation inspired by spatial filtering commonly used in radio astronomy. In section II, we present a model for

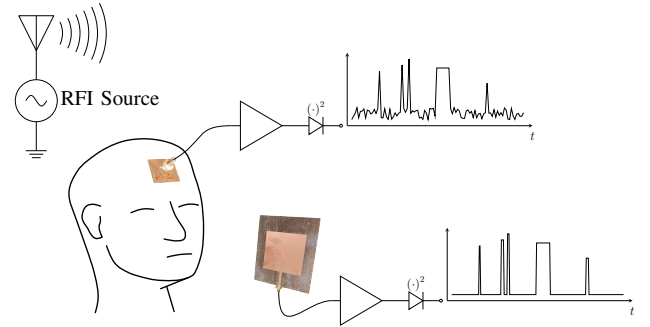


Fig. 1. Radiometer measuring brain temperature with an interferer transmitting a pulse train. Pulses are received by the radiometer as RFI. The RFI reference antenna is placed within the coherence wavelength of the temperature probe, which is inversely proportional to the bandwidth of the receiver.

estimating the correlation between two signals and validate the model using simulation. In section III, the model is validated in a simple simulated experimental scenario.

## II. INTERFERENCE MODELLING

For this work, a 1.4-GHz radiometer is chosen as a compromise between antenna size and sensing depth. Although this is a quiet band, the surrounding spectrum is densely allocated, and example measurements in an urban environment can be found in, e.g., [10]. In-band interference can be due to harmonics from transmitters at lower frequencies, transmitters in the adjacent bands, or unintentional radiators in the environments. For wearable applications, a technique to mitigate interference is desired which is real-time and can run on modest compute resources (such as a micro-controller).

Numerous techniques already exist for interference detection, suppression, and cancellation. For interference detection, statistical tests such as a kurtosis or the Shapiro-Wilk test are preferred [11], [12]. Once RFI detection is performed, time and/or frequency blanking can be used to completely remove an interfering signal, at the cost of increasing integration time. Interference can be suppressed using tuneable filters, but these are lossy and the rejection is relatively weak [13]. Techniques which use additional “auxiliary” antennas have also been implemented. Spatial filtering is used extensively in radio astronomy [14], and an adaptive filter has been demonstrated for interference cancellation in microwave thermometry [9]. Spatial filtering for interfering emitters that are spatially separated from the desired signal source can be effective when a large number

of phased antenna elements are used, but is complex and computationally expensive. This prohibits implementation in embedded systems. While adaptive filters are relatively simple, they suffer from similar computation issues. Here, we take inspiration from spatial filtering and propose a new technique for estimating the amount of interference in a radiometric signal using a reference antenna and receiver, and then subtracting it.

#### A. Model for Thermal Noise with Super-Imposed RFI

Referring to Fig. 1, we assume a single interfering signal, an auxiliary antenna matched to free space, and a near-field antenna matched to human tissue on the forehead. As viewed from the output of a total power radiometer, the interferer produces pulses of RFI according to a statistical process, each pulse resembling a box-car function of variable width and height. The interfering statistical process is received by both the auxiliary antenna and the temperature sensing probe. Because the temperature sensing probe is matched to a lossy medium which has significantly higher permittivity than air, we assume that a fraction of the signal received by the auxiliary antenna is received by the probe. The temperature probe is measuring the temperature of the medium by receiving and detecting the noise power of black-body radiation.

We denote the measured signal from the temperature probe as  $S_t$ , which is the sum of a statistical thermal noise signal  $n$ , plus the RFI reference signal  $S_i$  (also statistical in this case) multiplied by a coupling coefficient  $c$ :

$$S_t = cS_i + n, \quad (1)$$

where  $n$  and  $S_i$  are assumed to be uncorrelated. The distribution of  $n$  depends on the radiometer architecture, but does not impact the following calculations. Our goal is to find an expression for  $c$ . This expression should take in to account the correlation of the signals  $S_t$  and  $S_i$ . A simple approach computes the covariance of  $S_t$  and  $S_i$  as:

$$\begin{aligned} \text{Cov}[S_i, S_t] &= \text{E}[(S_i - \mu_{S_i})(S_t - \mu_{S_t})] \\ &= \text{E}[(S_i - \mu_{S_i})(cS_i + n - \mu_{S_t})] \\ &= c(\text{E}[S_i^2] - \mu_{S_i}^2). \end{aligned} \quad (2)$$

We identify the coupling coefficient [15]:

$$c = \frac{\text{Cov}[S_i, S_t]}{\text{Var}[S_i]}. \quad (3)$$

Using (3) and (1), we can write estimate the original thermal signal as  $n' = S_t - cS_i$ . This approach is independent of sampling frequency and relies only upon synchronous sampling of the auxiliary and thermal signals and can be applied to any system where synchronous sampling is guaranteed. It is assumed that both reference and signal antennas receive RFI with no information delay, which implies they are physically separated by a distance much shorter than the coherence length  $\sim c_0/\Delta f$ , where  $c_0$  is the speed of light in vacuum and  $\Delta f$  the receivers' instantaneous bandwidths.

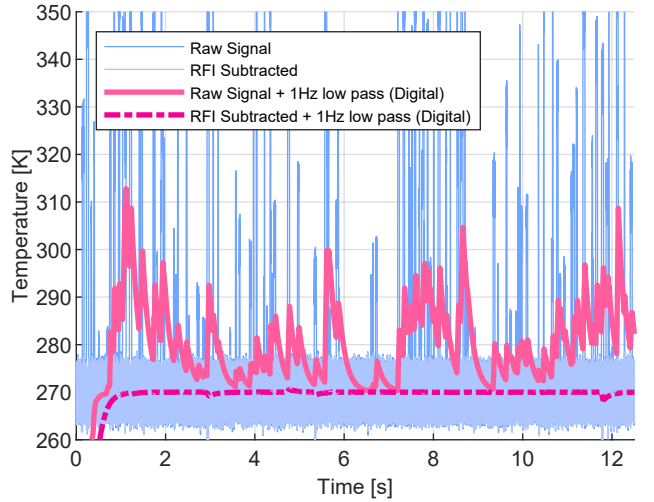


Fig. 2. Simulated radiometer output with a perfectly matched, 270 K load when a single interferer is present, with interference cancellation and low pass filtering applied. Here, the coupling coefficient between the interferer and radiometer is constant in time, however similar results can be obtained when the coupling coefficient varies by adjusting the rate at which the coupling coefficient is estimated.

#### B. Simulated Results

A simulation model for RFI is developed using MATLAB to test the technique. Seen by a radiometer, RFI appears as an effective temperature increase for some duration of time. A rectangular pulse with a uniformly distributed duration and amplitude is assumed. The arrival of each pulse is modeled using an exponential random process with rate  $\lambda$  [16]. In our simulation, the interfering random signal follows (1), where the coupling coefficient is constant. Note that for multiple and moving sources the coupling coefficient is not constant. The thermal noise signal is picked from  $\mathcal{N}(T_0, T_0/\sqrt{2B\tau})$  for each sample and receiver bandwidth  $B$ , integration time  $\tau$ , and mean antenna temperature  $T_0$ . Note that the exact distribution of the noise does not matter, as shown in (2). To estimate the correlation coefficient, we split the data set into a series of "windows" with adjustable widths. The coupling coefficient is then estimated using (2) over each finite window.

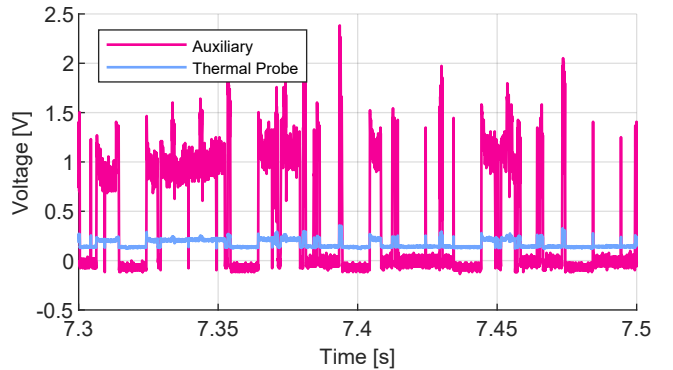


Fig. 3. Measured raw data from the receivers connected to the thermometer antenna and the auxiliary RFI sensing antenna (Fig. 1). Note that the radiometric signal contains interference which is highly correlated with the reference signal. The auxiliary signal dc offset is corrected.

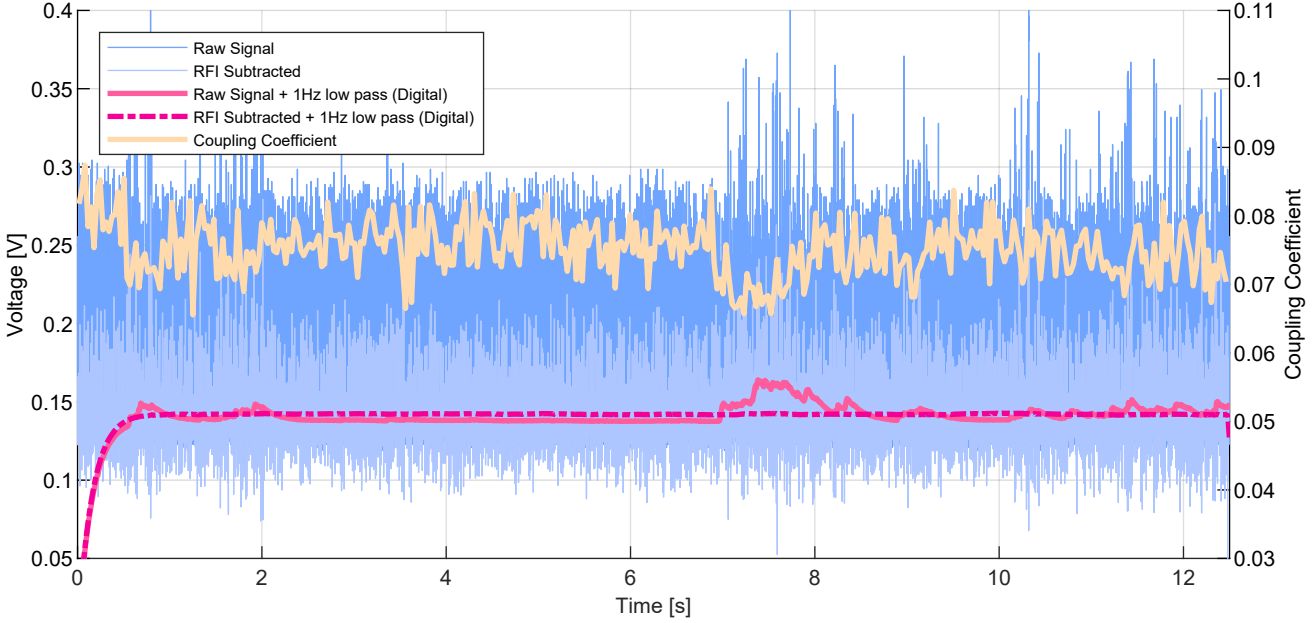


Fig. 4. Measured radiometer output with and without post processing. Simple RFI subtraction is shown for comparison and does not help significantly. A low pass filter applied on the radiometer output produces a fluctuating signal, which corresponds to tens of degrees, see Fig. 5. Compared to the RFI subtraction technique with a low pass filter, the output is nearly constant. The coupling coefficient defined by (3) is also shown.

A simulation of a desired signal infected by RFI is shown in Fig. 2. RFI pulse arrival rates of  $\lambda = 10$  Hz and pulse widths in the range 0–50 ms with amplitudes corresponding to 20 K–900 K are chosen. The coupling coefficient for each pulse is chosen to be  $c = 0.1$ . The simulated sampling rate is 150 kHz ( $\Delta f = 75$  kHz video bandwidth). The window width of 5000 samples (33.3ms) is used for this simulation. The temperature of the thermal source is 270 K. In this simulated case, the subtraction algorithm works well to eliminate RFI, producing a steady 270 K at the output.

### III. MEASUREMENT

Measurements are performed in an anechoic chamber using two shielded 1.4-GHz receivers, each with 44-dB gain followed by filters to select the band of interest. The signal is then detected using a biased diode detector. Post detection gain of the dc signal is performed using a trans-impedance amplifier, followed by a difference amplifier. The receivers are powered using a battery and a linear regulator.

A cell phone interferer is placed in the chamber. One of the receivers is connected to a near-field radiometric probe antenna on a stack of Play-Doh, which has been found experimentally to be a good analog for human muscle tissue [8]. The other receiver is connected to a 1.4 GHz patch antenna pointed towards the interferer, with some attenuation to prevent the detector from saturating. The output of the detector is captured by an oscilloscope over a period of 12 sec with a sample rate of 154 ksps. The raw data from the auxiliary and thermal probe is shown in Fig. 3. We observe that the RFI reference

signal is highly correlated with the interference observed in the radiometric measurement.

As in the simulation, the correlation coefficient is estimated by splitting the data into windows, each 5000 samples wide. It is important to note that (2) implicitly assumes that the dc level of the auxiliary receiver, when no interference is present, is zero since (2) cannot account for dc offsets. To correct for the dc offset of a real receiver in the auxiliary antenna, it is subtracted during data processing. Practically, the offset can be obtained using a Dicke switching circuit.

A digital low-pass filter with a 1-Hz knee is used to average the results and is implemented following:

$$V_n = \beta V_{n-1} + (1 - \beta)v_i \quad (4)$$

where  $v_i$  is the input signal,  $V_{n-1}$  is the previous filtered signal,  $\beta = e^{-\omega_0 T_s}$ ,  $\omega_0$  is the knee frequency, and  $T_s$  is the sampling period [17]. The knee of the low pass filter is also a free variable and can be tuned. The result of the RFI subtraction and filtering is shown in Fig. 4.

To estimate the temperature error, the RFI-free dc signal is subtracted from the signal of interest. The resulting voltage variation is then multiplied by the receiver sensitivity, estimated in each case as (300 K) / (dc level in V). Since each signal displays variation in the RFI-free dc level—which we attribute to LNA gain fluctuations—a different sensitivity is calculated in each case. The temperature error of the unprocessed thermal signal and signal with subtracted RFI are plotted in Fig. 5. To compare with the RFI-free fundamental radiometric uncertainty, measurements with the receiver input connected to a room-temperature matched termination are

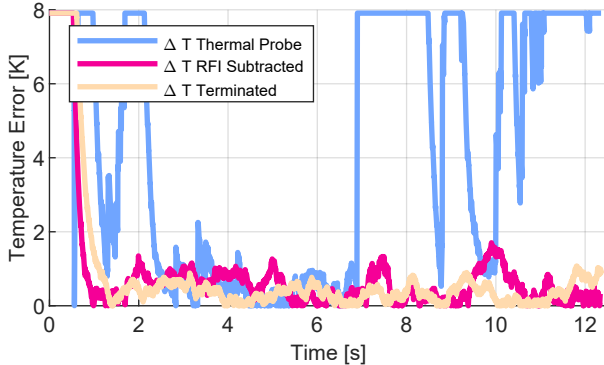


Fig. 5. Temperature error comparison for a measurement over about 12 sec. The highest error reported is 56 K, which occurs at about 8 sec. Each signal has been processed with a 1 Hz knee low-pass filter. The thermal probe has a standard deviation of 3.5 K, while the subtracted signal shows a standard deviation of 0.38 K. This is comparable to the reference case which has a standard deviation 0.22 K calculated from 2–12 seconds.

included. Without RFI subtraction, we can see that the unprocessed thermal probe signal displays significant jumps in temperature, with the peak occurring at about 8 seconds with a delta of 56 K. The standard deviation of the unprocessed signal is 3.5 K. With RFI subtraction, we obtain better than a 2 K variation over 12 seconds, and a standard deviation of 0.38 K; which is comparable to the variation in the terminated case which displays at most 1 K variation over 12 seconds, and a standard deviation of 0.22 K.

#### IV. CONCLUSION

We present and validate a simple technique for interference cancellation for passive microwave thermometry, using an auxiliary RFI reference antenna. The efficacy of the approach is demonstrated by comparison to baseline thermal measurements. The proposed interference cancellation algorithm can almost completely remove the effects of an interferrer, while performing only amplitude correlations of the received signals. We are able to achieve a standard deviation in the subtracted signal of 0.38 K, which is comparable to the fluctuations of a radiometer with a reference load with a corresponding standard deviation of 0.22 K. This is a dramatic improvement compared to the unprocessed signal which shows a standard deviation of 3.5 K.

Due to the directional nature of RFI, it is desirable to extend equation (2) to multiple auxiliary antennae. This can be done by recursive RFI subtraction for each of  $n$  antennae. The corresponding signals are  $S_{i,j}$  for  $j \in [1, n]$  and a recurrence relation to estimate the noise signal can be formed as:

$$n'_j = n'_{j-1} - c_j S_{i,j} , \quad (5)$$

where the final estimate for the noise signal is  $j = n$ . The coupling coefficient  $c_j$  is then calculated between the estimate  $n'_{j-1}$  and the auxiliary signal  $S_{i,j}$ . It is important to note that one cannot simply calculate a coupling coefficient for each auxiliary signal, and then subtract. This would have the consequence of potentially "double counting" an interfering source. Thus, subtraction should be done recursively.

#### REFERENCES

- [1] A. S. Howe and B. P. Boden, "Heat-related illness in athletes," *The American journal of sports medicine*, vol. 35, no. 8, pp. 1384–1395, 2007.
- [2] K. L. Carr, "Microwave radiometry: Its importance to the detection of cancer," *IEEE Transactions on Microwave Theory and Techniques*, vol. 37, no. 12, pp. 1862–1869, 1989.
- [3] K. Maruyama, S. Mizushima, T. Sugiura, G. Van Leeuwen, J. Hand, G. Marrocco, F. Bardati, A. Edwards, D. Azzopardi, and D. Land, "Feasibility of noninvasive measurement of deep brain temperature in newborn infants by multifrequency microwave radiometry," *IEEE Transactions on Microwave Theory and Techniques*, vol. 48, no. 11, pp. 2141–2147, 2000.
- [4] M. Paulides, J. Bakker, M. Linthorst, J. Van der Zee, Z. Rijnen, E. Neufeld, P. Pattynama, P. Jansen, P. Levendag, and G. Van Rhoon, "The clinical feasibility of deep hyperthermia treatment in the head and neck: new challenges for positioning and temperature measurement," *Physics in Medicine & Biology*, vol. 55, no. 9, p. 2465, 2010.
- [5] F. Biancari, T. Juvonen, and G. Spezzale, "Commentary: Cooling the brain for elective aortic hemiarch repair," *J. Thoracic Cardiovascular Surg.*, May 2021.
- [6] S. G. Vesnin, M. K. Sedankin, L. M. Ovchinnikov, A. G. Gudkov, V. Y. Leushin, I. A. Sidorov, and I. I. Goryanin, "Portable microwave radiometer for wearable devices," *Sens. Actuators A, Phys.*, vol. 318, p. 112506, Feb. 2021.
- [7] J. Edrich and P. Hardee, "Thermography at millimeter wavelengths," *Proc. IEEE*, vol. 62, no. 10, pp. 1391–1392, Oct. 1974.
- [8] R. Streeter, "High-resolution deep-tissue microwave thermometry," Ph.D. dissertation, University of Colorado at Boulder, 2023.
- [9] P. Momenroodaki, "Radiometric thermometry for wearable deep tissue monitoring," Ph.D. dissertation, University of Colorado at Boulder, 2017.
- [10] M. Piñuela, P. D. Mitcheson, and S. Lucyszyn, "Ambient rf energy harvesting in urban and semi-urban environments," *IEEE Transactions on microwave theory and techniques*, vol. 61, no. 7, pp. 2715–2726, 2013.
- [11] R. D. De Roo, S. Misra, and C. S. Ruf, "Sensitivity of the kurtosis statistic as a detector of pulsed sinusoidal radio frequency interferer," in *2007 IEEE International Geoscience and Remote Sensing Symposium*, 2007, pp. 2706–2709.
- [12] B. Guner, M. Frankford, and J. T. Johnson, "On the shapiro-wilk test for the detection of pulsed sinusoidal radio frequency interference," in *IGARSS 2008 - 2008 IEEE International Geoscience and Remote Sensing Symposium*, vol. 2, 2008, pp. II-157–II-160.
- [13] D. Psychogiou, R. Gómez-García, and D. Peroulis, "A class of fully-reconfigurable planar multi-band bandstop filters," in *2016 IEEE MTT-S International Microwave Symposium (IMS)*, 2016, pp. 1–4.
- [14] B. Jeffs, L. Li, and K. Warnick, "Auxiliary antenna-assisted interference mitigation for radio astronomy arrays," *IEEE Transactions on Signal Processing*, vol. 53, no. 2, pp. 439–451, 2005.
- [15] A. Papoulis, *Probability, Random Variables, and Stochastic Processes*, 3rd ed. McGraw-Hill, Inc., 1991, ch. Moments and Conditional Statistics, pp. 152–153.
- [16] S. Ross, *A First Course in Probability*, 9th ed. Pearson, 2014, ch. Continuous Random Variables, pp. 197–198.
- [17] P. Horowitz and W. Hill, *The Art of Electronics*, 3rd ed. Cambridge University Press, 2021, ch. Digital Signal Processing, p. 419.